Research Journal of Applied Sciences, Engineering and Technology 7(11): 2362-2370, 2014
DOI:10.19026/rjaset.7.537
ISSN: 2040-7459; e-ISSN: 2040-7467

Submitted: August 08, 2013 Accepted: August 26, 2013 Published: March 20, 2014

Research Article

Deign of Experiment and Optimization of Plasma Transferred Arc Hardfacing on Structural Steel with Titanium Carbide

S. Balamurugan and N. Murugan
Department of Mechanical Engineering, Coimbatore Institute of Technology,
Civil Aerodrome (Post), Coimbatore 641014, India

Abstract: The aim of the Plasma Transferred Arc (PTA) hardfacing process is improving a technical surface locally with a dedicated material; Hardfacing became an issue of intense development related to wear resistant application. The hardfacing procedures can be differentiated by the intensity of mixture with the base body, which is usually increasing along with an increasing fusion efficiency rate. Nearly all kinds of weldable materials can be hardfaced and mostly all types of known wear resistant metals in combination can be used as hardfacing materials. The PTA hardfacing process has been widely employed due to several advantages such as higher volume of metal deposition rates and achieving very low dilution level. Heat input which influences dilution can be controlled by proper selection of PTA process parameters. In this study, an attempt has been made to analyze PTA hardfacing of IS: 2062 structural steel with Titanium Carbide (TiC). Experiments were conducted based on a fully replicable five-factor, five-level central composite rotatable design. Mathematical models were developed using response surface methodology to study the effects of PTA hardfacing process parameters such as welding current, welding speed ,powder feed rate, oscillation width and pre heat temperature on bead geometry parameters like penetration, reinforcement, bead width and dilution. Direct and interaction effects of PTA process parameters on bead geometry were analyzed. From mathematical model, the process parameters were optimized.

Keywords: Design of Experiments (DOE), effects, optimization, PTA hardfacing

INTRODUCTION

Wear related failure of mechanical components is considerable as one of the major reasons for inefficiency of a variety of engineering applications. It was reported that wear resistance could be improved when hard particles were embedded in a tough, metallic matrix (Jha *et al*., 1999; Draugelats *et al*., 1996). Hardfacing is a technique used to improve the surface properties of metallic mechanical parts, such as the resistance against wear and correction. Surface properties and quality depend upon the selected alloys and deposition processes (Davis and Davis & Associates, 1993; Lugscheider *et al*., 1991). Depending on the applied technique, common problems encountered in hardfacing are combination of a poor bonding of the applied surface layer to the base material, the occurrence of porosity of the thermal distortion of the workspiece, the mixing of the layer with the base material and the inability of a very local treatment (Wolfgang, 2012).

According to the literature, coatings obtained by PTA present a very good alternative to other hardfacing processes, such as conventional techniques or more recent ones like laser cladding (D' Oliveira *et al*., 2002; Agustin *et al*., 2011). A significant advantage of PTA surfacing over traditional surface welding processes arises from the fact that the consumable material used is in the powder form. This fact enables a wide range of composition for the coating materials and even mixtures of different material powders.

Hardfacing experiments are conducted using DOE which deals with the procedure of selecting number of trials and conditions for running those (Cochran and Cox, 1962). Using the results of the experiments to correlate welding process parameters to bead geometry and dilution, mathematical models can be developed for the corresponding welding process (Davis, 1983; Harris and Smith, 1983). These models can be used to automate the welding process which can be helpful for consistently producing high quality hardfacing with less demand on welder skills. Siva *et al*. (2009) deposited nickel based colmonoy overlays on stainless steel 316L by PTAW using five level central composite rotatable designs and the percentage of dilution was optimized. Amos Robert Jayachandrana and Murugana (2010) investigated on AISI 316 L stainless steel cladding of structural steel by using PTA process and studied bead geometry variables and claddings deposited at different heat input and at optimum dilution conditions. Mohan

Corresponding Author: S. Balamurugan, Department of Mechanical Engineering, Coimbatore Institute of Technology, Civil Aerodrome (Post), Coimbatore 641014, India

Table 1: Chemical composition of base metal and hardfacing alloy

	Elements, weight %							
Material used	C	Si	Mn	S	P	Mg	Ti	Fe
IS:2062 (base metal)	0.18	0.18	0.98	0.016	0.016	-	-	bal
Titanium Carbide (TiC) (PTA powder)	12.50	0.03	0.03	-	-	0.09	81.2	0.12

Table 2: Process control parameters and their limits

			Factor levels				
Parameters	Units	Notation	-2	-1	0	1	2
Welding current	amps	I	160	175	190	205	220
Welding speed	mm/min	S	120	130	140	150	160
Powder feed rate	g/min	F	12	14	16	18	20
Oscillation width	mm	H	8	9	10	11	12
Preheat temperature	°C	T	230	260	290	320	350

and Muragan (2009e) studied tungsten carbide hardfacing of stainless steel by PTA process. Very few works has been reported on TiC hardfacing. In this study, details about the development of mathematical models for predicting the direct and interaction effects of process parameter variables for TiC hardfacing on bead geometry and dilution from the experimental data obtained.

MATERIAL AND HARDFACING ALLOY

Selection of substrate materials: The substrate material selected for the PTA hardfacing method was IS: 2062 structural steel. The chemical composition of IS: 2062 structural steel and hardfacing alloy is presented in Table 1.

Plan of investigation: The research study was planned to be carried out in the following steps:

- Identifying the important process control variables and finding their upper and lower limits
- Developing the design matrix and conducting the experiments as per the design matrix
- Developing mathematical models
- Result and discussion-presenting the main effects and few significant interaction effects of different parameters in graphical form
- Conclusion

Identification of process control variables and finding their limits: The independently controllable process parameters were identified to enable the carrying out of the experimental work and the development of mathematical models: they are welding Current (I), welding Speed (S), powder Feed rate (F), oscillation width (H), preheat Temperature (T) identified as control variables. Trial runs were carried out with the bead laid on plates as well as by varying one of the process parameters whilst keeping the rest of them at constant values. The upper limits of the factors was coded as +2 and the lower limits as -2, the coded values for intermediate ranges are then calculated from the following relationship, $X_i = 2\,[2X - (X_{max} + X_{min})] / [X_{max} - X_{min}]$, where, X_i - the required coded value of a variable X ; X - any value of the variable from X_{max} to X_{min}; X_{min}- the lower level of the variable, X_{max}- the upper level of the variable. The decided levels of the selected process parameters with their units and notations are given in Table 2.

Fig. 1: Photograph of hardfaced plates

Developing the design matrix and conducting the experiments as per the design matrix: The design matrix chosen to conduct the experiment was a central composite rotatable design. It consists of 32 sets of coded conditions and comprising a half replication of $2^4 = 16$ factorial design with 6 centre points and 10 star points. All the welding parameters at the middle level (0) constitute centre points whereas the combination of each welding parameters at its lower value (-2) or higher value (2) with the other four parameters at the middle levels constitute the star points. Thus the 32 experimental runs allowed the estimation of linear, quadratic and two-way interactive effects of the process parameters on the weld bead geometry. The design matrix is shown in Table 3. The experiment was conducted as per the design matrix. The IS: 2062 Structural steel plate of size 150×100×20 mm is to be hardfaced by PTA system. The Titanium Carbide (TiC) powder having size of 50-100 µm was deposited by PTA hardfacing process on structural steel plates. It is shown in Fig. 1.

The hardfaced plates were cross-sectioned at their mid points to obtain test specimens. The specimens were prepared by the usual polishing method and etched with 2% nital. The weld bead profiles were

Table 3: Design of matrix and observed values of weld bead geometry

	Design matrix					Bead geometry			
Sl. No.	I	S	F	H	T	P (mm)	R (mm)	W (mm)	Dilution (%)
1	-1	-1	-1	-1	1	1.31	1.70	09.38	31.70
2	1	-1	-1	-1	-1	1.60	1.83	10.58	34.49
3	-1	1	-1	-1	-1	1.36	1.45	09.37	26.28
4	1	1	-1	-1	1	1.27	1.84	10.50	40.00
5	-1	-1	1	-1	-1	1.35	1.92	10.60	27.24
6	1	-1	1	-1	1	1.25	1.42	09.86	38.08
7	-1	1	1	-1	1	0.83	1.05	09.27	28.66
8	1	1	1	-1	-1	1.49	2.09	10.53	30.18
9	-1	-1	-1	1	-1	1.37	1.84	11.43	35.92
10	1	-1	-1	1	1	1.08	1.28	10.89	44.84
11	-1	1	-1	1	-1	1.25	1.80	10.84	27.84
12	1	1	-1	1	1	1.00	1.43	10.72	38.96
13	-1	-1	1	1	1	2.09	2.16	11.32	45.12
14	1	-1	1	1	-1	1.68	2.20	11.18	37.77
15	-1	1	1	1	-1	1.12	1.60	11.04	29.95
16	1	1	1	1	1	1.28	1.98	10.91	41.10
17	-2	0	0	0	0	0.99	1.19	11.20	36.11
18	2	0	0	0	0	1.00	1.41	11.12	46.03
19	0	-2	0	0	0	0.85	1.32	11.77	29.81
20	0	2	0	0	0	1.13	2.21	13.85	38.89
21	0	0	-2	0	0	0.87	1.01	10.18	31.71
22	0	0	2	0	0	0.92	1.16	09.83	21.95
23	0	0	0	-2	0	0.67	1.31	08.46	15.64
24	0	0	0	2	0	1.43	1.65	11.12	35.32
25	0	0	0	0	-2	1.11	1.81	11.30	30.96
26	0	0	0	0	2	1.26	1.22	11.00	40.84
27	0	0	0	0	0	1.22	1.36	11.83	41.65
28	0	0	0	0	0	1.07	1.05	11.71	41.71
29	0	0	0	0	0	1.15	1.46	12.25	40.98
30	0	0	0	0	0	1.42	1.55	12.38	39.29
31	0	0	0	0	0	1.21	1.54	11.94	41.34
32	0	0	0	0	0	1.32	1.38	11.61	41.44

I: Welding current (amps); S: Welding speed (mm/min); F: Powder feed rate (g/min); H: Oscillation width (mm); T: Pre heat temperature (°C); P: Penetration (mm); R: Reinforcement (mm); W: Width (mm), D: Dilution (%)

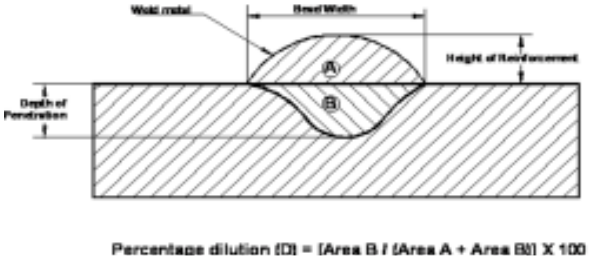

Fig. 2: Cross-section of weld bead geometry

traced using a profile projector and the bead geometry and areas of the penetration and reinforcements were measured. The bead profile and area of the penetration and reinforcement of a typical bead are shown in Fig. 2.

DEVELOPMENT OF MATHEMATICAL MODELS

The response function representing any of the weld bead dimensions like penetration, reinforcement, width and dilution etc can be expressed as:

$$Y = f(I, S, F, H, T)$$

where,
Y = The response

The second order polynomial (regression) used to represent the response surface for k factors is given by technique was employed to determine significant coefficients. The final mathematical model was constructed using the significant coefficients. The final mathematical models determined by the regression analysis are as follows:

$$P = 1.161 - 0.029\ I - 0.049\ S + 0.097\ H + 0.112\ T + 0.059\ T^2 + 0.084\ I\ F - 0.14\ I\ H - 0.1\ I\ T - 0.098\ S\ F + 0.106\ F\ H + 0.132\ H\ T$$

$$R = 1.343 + 0.07\ I + 0.065\ F + 0.07\ H - 0.17\ T + 0.145\ S^2 + 0.074\ H^2 + 0.083\ T^2 + 0.188\ I\ S + 0.121\ F\ H$$

$$W = 11.992 + 0.565\ H - 0.238\ I^2 + 0.175\ S^2 - 0.526\ F^2 - 0.58\ H^2 - 0.24\ T^2 - 0.38\ I\ H + 0.218\ S\ T - 0.174\ F\ T + 0.184\ H\ T$$

$$\%\ D = 40.529 + 2.548\ I + 3.51\ H + 2.848T - 0.928\ S^2 - 0.525\ F^2 - 3.145\ H^2 - 1.213\ S\ H$$

The adequacies of the developed models were tested using ANOVA and it was found that all models converge adequate. The estimated R^2 values of the

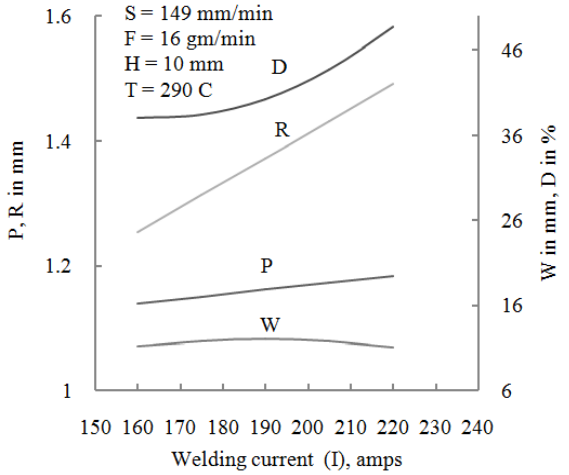

Fig. 3: Direct effects of welding current on bead geometry

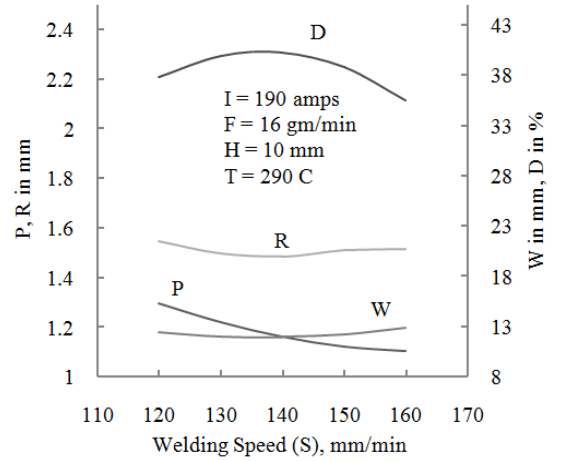

Fig. 4: Direct effects of welding speed on bead geometry

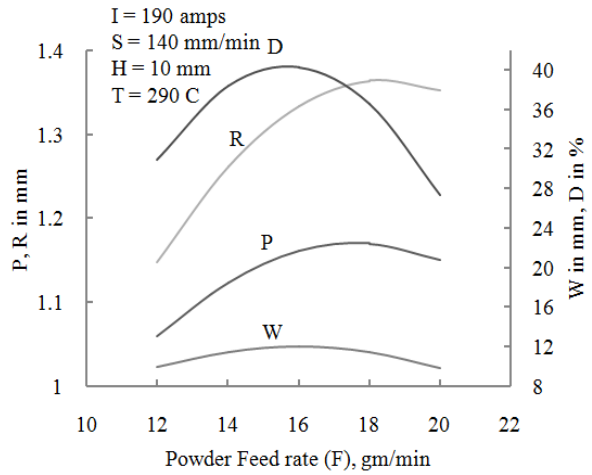

Fig. 5: Direct effects of powder feed rate on bead geometry

models P, R, W and % of D are respectively 0.618, 0.686, 0.793 and 0.521.

RESULTS AND DISCUSSION

Direct effects of process parameters on bead geometry:

Effects of welding current on bead geometry: The effect of welding current on bead geometry is presented in Fig. 3. From the figure, it is found that the P, R, D increase with increase in welding current. This is attributed to the fact that heat input to the base metal increases when I is increased. W is not significantly affected by I:

$$Y = b_0 + \sum_{i=1}^{k} b_i x_i + \sum_{i=1}^{k} b_{ii} x_i^2 + \sum_{i,j=1, j\neq i}^{k} b_{ij} x_i x_j$$

where, b_0 is the free term of the regression equation, the coefficients b_1, b_2,… b_k are linear terms, the coefficients b_{11}, b_{22},…b_{kk} are quadratic terms and coefficients b_{12}, b_{13},….$b_{k-1,k}$ are the interaction terms. For five factors, the selected polynomial could be expressed as:

$$Y = b_0 + b_1 I + b_2 S + b_3 F + b_4 H + b_5 T + b_{11} I^2 + b_{22} S^2 + b_{33} F^2 + b_{44} H^2 + b_{55} T^2 + b_{12} I S + b_{13} IF + b_{14} IH + b_{15} IT + b_{23} S F + b_{24} SH + b_{25} ST + b_{34} FH + b_{35} FT + b_{45} HT$$

The values of the coefficient of the above polynomial were calculated by regression analysis with the help of the QA Six Sigma DOE IV PC software package. From the calculated coefficient of the polynomial less significant coefficient was eliminated with the help of back elimination.

Effects of welding speed on bead geometry: The effect of welding speed on bead geometry is presented in Fig. 4. From the figure, it is found that the P decreases with increase in S. This could be attributed to the reduction in heat input per unit length of weld bead when S is increased. R decreases initially with the increase in S and then it is not affected with the further increase in S. W is not significantly affected. Dilution, D increases with an increase S to a maximum value and then decreases with the further increase in S. This is because of the initial reduction in R, D increases. Further decrease in D may be due to continuous reduction in P.

Effects of powder feed rate on bead geometry: Figure 5 shows the effect of powder Feed rate (F) on bead geometry. From the figure, it is found that P increases with the increase in F. This is because less heat of plasma is utilized for melting of powder when F is less. R increases with the increase in F. This may be due to the consumption of more arc energy for melting powder. D increases to a maximum value when F increases and then D decreases with the further increase

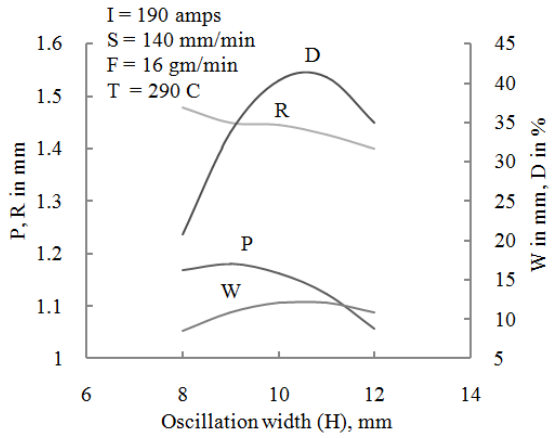

Fig. 6: Direct effects of oscillation width, (H), mm

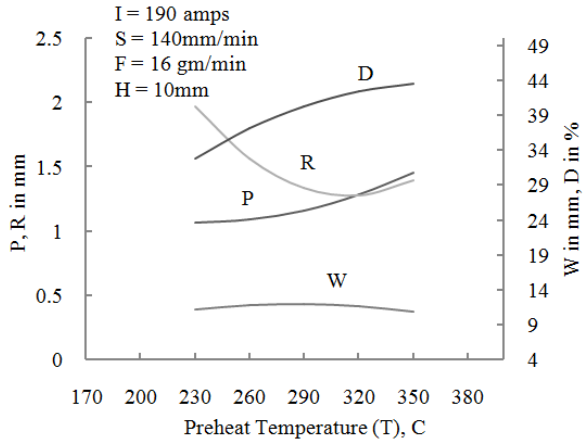

Fig. 7: Direct effects of preheat Temperature (T), C

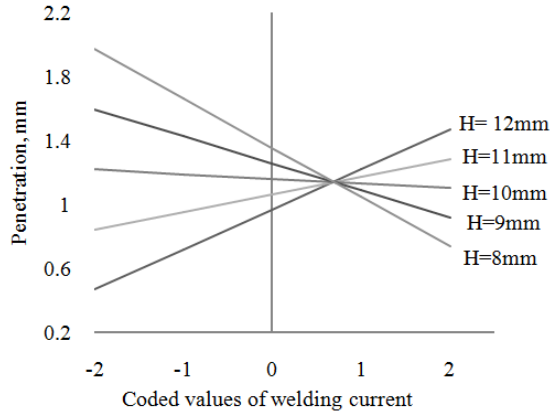

Fig. 8: Interaction effects of I and H on P

in F. This may be due to initial increase in P decrease in P when F increases. W is not affected significantly.

Effects of oscillation width on bead geometry: The effect of oscillation width on bead geometry is presented in Fig. 6. From the figure, it is found that P & R decrease with increase in H. This could be possibly due to the fact that the deposited metal got distributed along the width resulting in decrease in P & R. W increases with increase in H. This is because of the spreading of metal. D increases with increase in F reaching a maximum value and D deceases with further increase in H. This may be the effect of decrease in R.

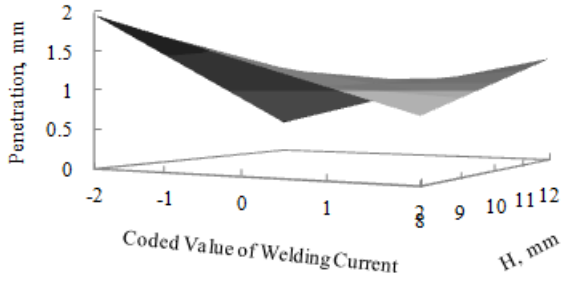

Fig. 9: Response surface showing interaction effects of I and H on P

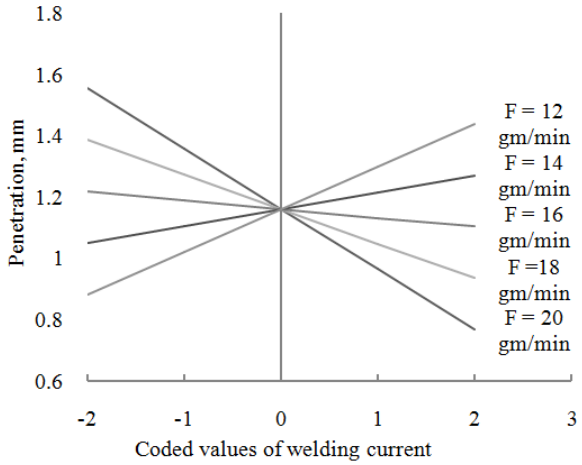

Fig. 10: Interaction effects of I and F on P

Effects of preheat temperature on bead geometry: The effect of preheat temperature on bead geometry is presented in Fig. 7. From the figure, it is found that P&D increase with increase in T. This could be attributed to the following: When T increases more melting of base metal occurs resulting in higher penetration and dilution. R decreases when T increases. This is may be due to the spreading of molten metal when T increases. W is not significantly affected by T.

Interaction effects of process parameters on bead geometry:

Effects of process variables on welding current and oscillation width on penetration: The interaction effect of welding current and oscillation width on penetration is presented in Fig. 8. From the figure, it can be observed that P increases with the increase in I when H is above 10 mm and P decreases with the

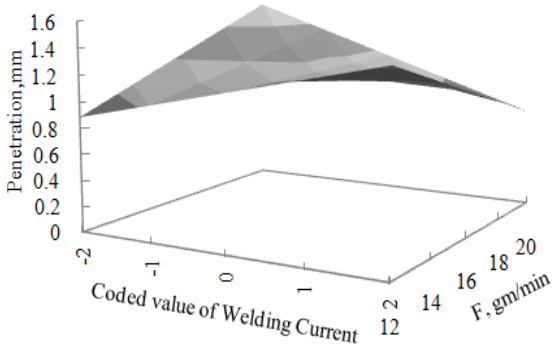

Fig. 11: Response surface showing interaction effect of I and F on P

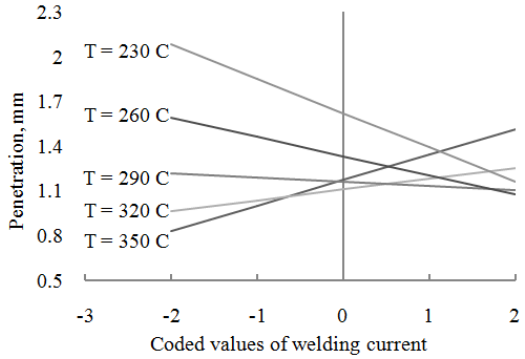

Fig. 12: Interaction effects of I and T on P

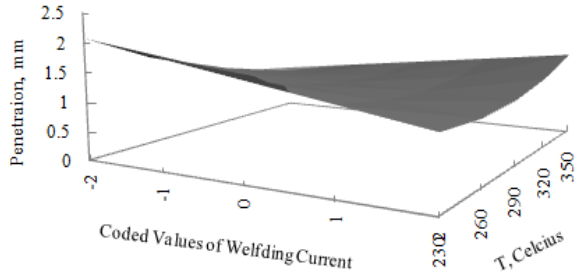

Fig. 13: Response surface showing interaction effects of I and T on P

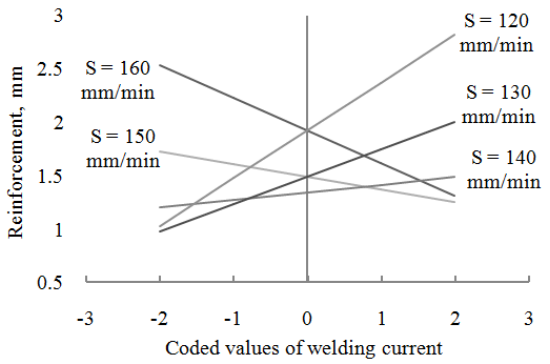

Fig. 14: Interaction effects of I and S on R

increase in I when H is blow 10 mm. The increase in P with the increase in I at higher oscillation width may be due to increase in heat input resulting in more melting of base metal causing higher penetration. The interaction effects are further visualized using response surface diagram as shown in Fig. 9.

Effects of process variables on welding current and powder feed rate on penetration: The interaction effect of welding current and powder feed rate on penetration is presented in Fig. 10. It is clear from the figure that the penetration increases with an increase in welding current when powder feed rate is below 16 g/min. This is due the fact that at lower volume flow rate of the metal powder more heat is available to fuse the base metal resulting in higher penetration. At higher powder feed rate more heat of plasma arc is consumed by powder for its melting resulting in lower melting of base metal. The interaction effects are further visualized using response surface diagram as shown in Fig. 11.

Effects of process variables on welding current and preheat temperature on penetration: The interaction effect of welding current and preheat temperature on penetration is presented in Fig. 12. It is clear from the figure that P increases in I for when T is above 290°C and P decreases with increase in I when T below 290°C. The increase in P with the increase in I at higher preheat temperatures may be due to increase in heat input and fluidity of molten metal resulting more melting of substrate. The interaction effects are further visualized using response surface diagram as shown in Fig. 13.

Effects of process variables on welding current and welding speed on reinforcement: The interaction effect of welding current and welding speed on reinforcement is presented in Fig. 14. It is clear from the figure that the R increases with the increase in I when S is below 150 mm/min, but it is also noted that the R decreases with the increase in I when S is above 140 mm/min. The increase in R with the increase in I at lower welding speed is attributed to the fact that heat input increases when I increases resulting in more melting of base metal. At higher welding speed metal deposition per unit length of welds decreases resulting in lower R. The interaction effects are further visualized using response surface diagram as shown in Fig. 15.

Effects of process variables on welding current and oscillation width on width: The interaction effect of welding current and oscillation width on width is presented in Fig. 16. It is clear from the figure that width increases with the increase in I when H is below 11 mm, but the trend reverses when H is above 10 mm. The increase in W at lower H may be due to increase in

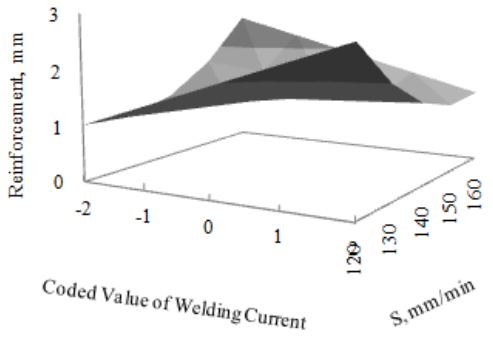

Fig. 15: Response surface showing interaction effects of I and S on R

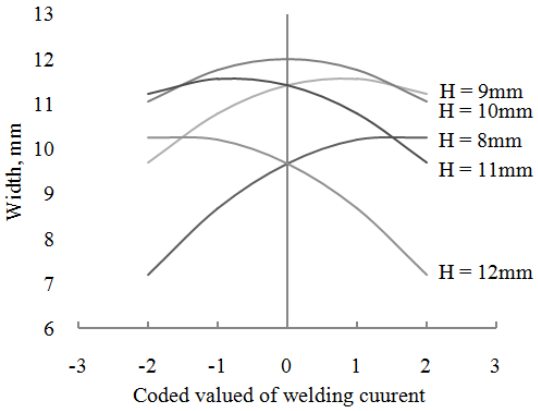

Fig. 16: Interaction effects of I and H on W

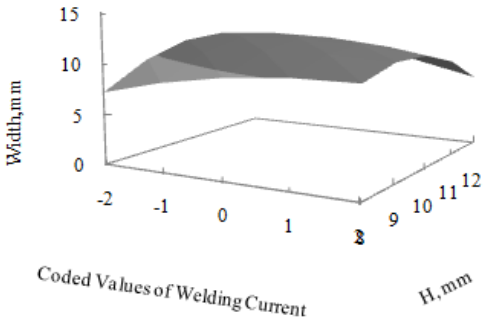

Fig. 17: Response surface showing interaction effect of I and H on W

heat input resulting more melting of base metal. When H is higher penetration increases with the increase I causing reduction in W. The interaction effects are further visualized using response surface diagram as shown in Fig. 17.

Effects of process variables on welding speed and powder feed rate on penetration: The interaction effect of welding speed and powder feed rate on penetration is presented in Fig. 18. It is evident from the

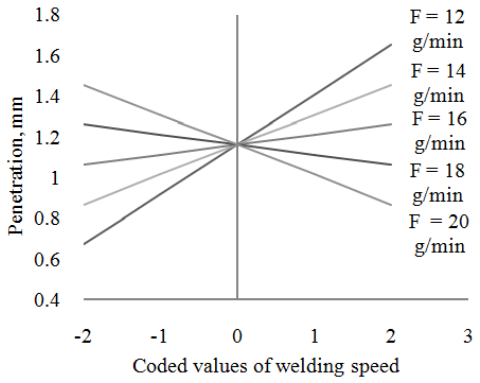

Fig. 18: Interaction effects of S and F on P

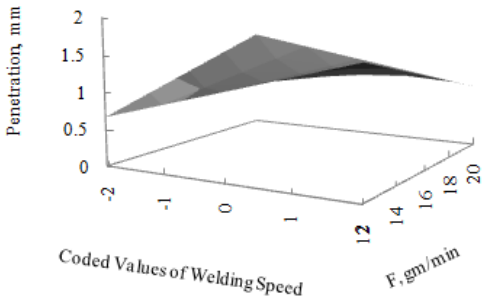

Fig. 19: Response surface showing interaction effect of S and F on P

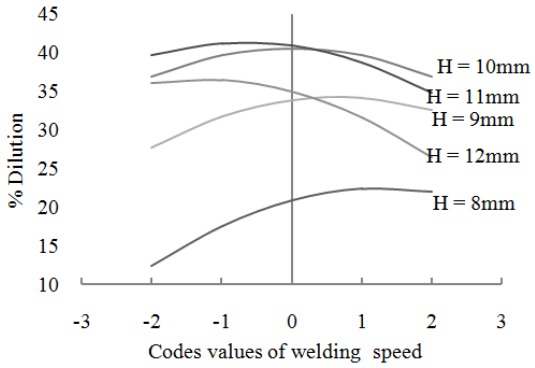

Fig. 20: Interaction effects of S and H on D

figure that when F is lower value, P increases with increase in S. It is because less heat of plasma is utilized for melting of powder when powder flow rate is less. The reverse trend is observed, when F increases to higher values. When F is increased more arc energy is consumed in melting the powder and P decreases. The interaction effects are further visualized using response surface diagram as shown in Fig. 19.

Effects of process variables on welding speed and oscillation width on % dilution: The interaction effect of welding speed and oscillation width on dilution is presented in Fig. 20. It is seen from the figure that D

Table 4: Optimized PTA hardfacing process parameters and corresponding bead geometry

Optimized factors		Optimized bead geometry			
I (amps)	220	P (mm)	R (mm)	W (mm)	D (%)
S (mm/min)	160	1.00	1.98	11.00	28.26
F (g/min)	16	Actual bead geometry			
H (mm)	12	P (mm)	R (mm)	W (mm)	D (%)
T (°C)	350	0.98	2.0	11.17	27.93
		% error			
		-2	1	1.56	-1.17

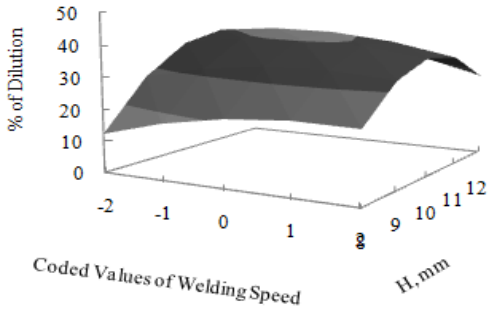

Fig. 21: Response surface showing interaction effect of S and H on D

initially increases with increase in S and then decreases with the further increase in S at all levels of H except H = 12 mm. At lower H when S increases P increases resulting in increased D. The interaction effects are further visualized using response surface diagram as shown in Fig. 21.

Optimization: The optimization was carried out using Microsoft Excel software. Solver is part of a suite of commands with what if analysis tools. Solver works with a group of cells that are related, either directly or indirectly, to the formula in the target cell. Solver adjusts the values in the changing cell, called the adjustable cells to produce the result. Constrains are applied to restrict the values of the variables used in the objective function.

- **Minimizing depth of penetration:** Optimum process parameters:

  I = +2 (220 amps); S = +2 (160 mm/min)
  F = +1 (18 g/min); H = -2 (8 mm)
  T = +1 (320°C)
  Predicted Response; P = 0.912 mm

- **Maximizing the reinforcement:** Optimum process parameters:

  I = +2 (220 amps); S = +2 (160 mm/min)
  F = 0 (16 g/min); H = -2 (8 mm)
  T = +1 (320°C)
  Prediced Response: R = 2.07 mm

- **Maximizing the bead width:** Optimum process parameters:

  I = +2 (220 amps); S = +1 (150 mm/min)
  F = +1 (18 g/min); H = +2 (12 mm)
  T = +1 (320°C)
  Predicted Response: W = 11.24 mm

- **Minimizing the % of dilution:**

  I = - 1 (175 amps); S = +2 (160 mm/min);
  F = +1 (18 g/min); H = -22 (8 mm);
  T = -1 (260°C)
  Predicted Response: %D = 27.12

- **Optimizing the bead geometry:** From the above iteration, the bead geometries were optimized with the following constrains and the factor levels were found out for this optimized condition. The constrains are as follows.
  Further optimized the process:

  p≤1.2; Peridicted Response: P = 1.13 mm
  R≥2; Peridicted Response: R = 2.04 mm
  W≥11; Peridicted Response: W = 11.20 mm
  % D≤30; Predicted Response: % D = 27.86

The experiment was conducted by setting the optimized by setting the optimized parameters. A comparison was made between the predicted and actual values of dilution and it was found that the average error is less than 2%. The results of the test with the optimum process parameters are presented in Table 4.

CONCLUSION

The following conclusions were arrived at from the above investigation:

- A five level factorial technique can be employed easily for developing mathematical models for predicting weld bead geometry within the limits of the process parameters applied for TiC hardfacing of structural steel.
- Reinforcement and dilution are increased when welding current is increased but penetration marginally increased when welding current is increased.
- Penetration and, dilution decrease when travel speed is increased. Reinforcement decreases initially with the increase in S.

- When the powder feed rate is increased, reinforcement is increased and subsequently dilution is decreased. When preheat temperature is increased penetration and dilution increase, whereas reinforcement decreases.
- Reinforcement and penetration are decreased with increases in H. D initially increases with increase in H and D decreases with the further increase in H
- Two way interactive effects of welding variables are found to be significant.
- In an optimization of objective process parameter functions are aimed for minimizing penetration and dilution and maximizing reinforcement and weld bead with. The results obtained are satisfactory.

REFERENCES

Agustin, G., G.S. Hernán, S.S. Estela and A.D.V. Luis, 2011. Effect of welding procedure on wear behavior of a modified martensitic tool steel hardfacing deposit. Mater. Des., 31(9): 4165-4173.

Amos Robert Jayachandrana, J. and N. Murugana, 2010. Investigation on the influence of surfacing process parameters over bead properties during stainless steel cladding. Mater. Manuf. Process., 27(1): 69-77.

Cochran, W.G and G.M. Cox, 1962. Experimental Design. Asia Publishing House, Bombay, India.

Davis, O.L., 1983. The Design and Analysis of Industrial Experiments. Longmoun, New York.

Davis, J.R. and Davis & Associates, 1993. Hardfacing, Weld Cladding and Dissimilar Metal Joining ASM Handbook: Welding, Brazing and Soldering. 10th Edn., ASM Metals Park, OH, 6: 699-823.

D' Oliveira, A.S.C.M., A.E. Yaedu and P.S.C.P. da Silva, 2002. Influence of dilution on microstructure and mechanical properties of cobalt-based alloy deposited by Plasma Transferred Arc Welding. Proceeding of the International Conference on Advanced Materials, Their Processes and Applications, Materials Week, Muchen.

Draugelats, U., *et al*., 1996. Weld Res. Abroad, 42(11): 39-41.

Harris, P. and B.L. Smith, 1983. Factorial technique for weld quality prediction. Metal Constr., 15(11): 661-666.

Jha, A.K., B.K. Prasad, R. Dasgupta and O.P. Modi, 1999. Influence of material characteristics on the abrasive wear response of some hard facing alloys. J. Mater. Eng. Perform., 8(2): 190-196.

Lugscheider, E., U. Morkramer and A. Ait-Mekideche, 1991. Advances in PTA surfacing. Proceeding of the 4th National Thermal Spray Conference, Pittsburgh, PA, USA.

Mohan, K. and N. Muragan, 2009. Effects of plasma transferred arc welding parameters on bead geometry in tungsten carbide hard facing. Int. J. Manuf. Sci. Prod., 10(3-4): 155-168.

Siva, K., *et al*., 2009. Studies on nickel based colmonoy overlays deposited on stainless steel 316L by plasma transferred arc welding. Int. J. Adv. Manuf. Technol., 41: 24-30.

Wolfgang, W.S., 2012. Trends for Hardfacing. Retrieved from: www.engineers.org.il/ uploads/ 1683/drwhal0206.pdf.